Supplementary information

High-throughput selection of sperm with improved DNA integrity and rapidly progressive motility using a butterfly-shaped chip compared to Swim-Up method

Ali Sharafatdoust Asl,[a] Mohammad Zabetian Targhi,[*a] Soroush Zeaei,[a] Iman Halvaei,[b] Reza Nosrati[*c]

[a] *Department of Mechanical Engineering, Tarbiat Modares University, Tehran, Iran.*

[b] *Department of Anatomical Sciences, Tarbiat Modares University, Tehran, Iran.*

[c] *Department of Mechanical and Aerospace Engineering, Monash University,*

Table S1. Comparison of microfluidic chip performance designed to enhance sperm biological parameters, progressive motility, motility, DNA improvement, having sperm collection, concentration, and separation time.

Microfluidics Device	Mechanism of Separation	Advantage	Motility (%)	Advantage	Sperm Collection	Advantage	Time (min)
		Progressive Motility – Selecting of (RP+SP)		DNA integrity (Improvement)		Concentration (10^6 Sperm cells/mL)	
Sarbandi et al.[1]	Rheotaxis	NA	100	NA	-	-	15
Sharma et al.[2]	Rheotaxis	NA	99.47	NA	+	-	60
Vasilescu et al.[3]	Boundary-following behavior	NA	95.5	1.4	+	5.5	20
Zaferani et al.[4]	Rheotaxis	NA	100	NA	-	-	5
Wu et al.[5]	Rheotaxis	+	93	NA	-	0.2	15
Heydari et al.[6]	Rheotaxis	NA	100	NA	-	-	15
Tasoglu et al.[7]	Motility	NA	NA	NA	+	-	5min- 1hr
Butterfly-shaped chip (Present work)	Rheotaxis-Boundary following behavior	94.9% (66.9%+28%)	95.9%	3.4% (80.5%)	+	4.1	Up to 20

I. Velocity difference rate between the channels

For the rheotaxis movement of sperm within the guiding arrays, the velocity profile inside the channels must be uniform to ensure that sperm are subjected to consistent velocities. Within the guiding arrays, each channel has a specific maximum velocity. The difference in these maximum velocities is used to assess the uniformity of flow within the channels. Variations in velocity among the channels help calculate the optimal values for different input angles and the number of arrays (ranging from 2 to 5) using the following equation:

$$\text{Max } V_{max}\left(\text{Between: } V_{max,C1}, V_{max,C2}, V_{max,C3}, V_{max,C4}, \text{or more}\right) = V_1 \quad \text{(S1)}$$

$$\text{Min } V_{max}\left(\text{Between: } V_{max,C1}, V_{max,C2}, V_{max,C3}, V_{max,C4}, \text{or more}\right) = V_2 \quad \text{(S2)}$$

$$\text{Difference velocity rate (\%)} = \frac{V_1 - V_2}{V_1} \times 100 \quad \text{(S3)}$$

According to Table S2, the number of arrays, ranging from two to five in various chips, is shown at five different angles by analyzing the differences in velocity rates. The ideal design

dimensions are led by a chip with 3 arrays (4 channels) at a 60-degree angle, as the minimal disparity signifies the consistency of velocity throughout all channels.

Table S2. Difference velocity rate for rotation angle and number of different arrays between 2 and 5 arrays in guiding arrays.

Number of arrays	Angle (α), Degree				
	15	30	45	60	75
2	28.71	22.24	17.93	13.23	38.56
3	17.97	15.82	9.12	4.93	23.34
4	20.52	19.37	14.9	7.01	34.33
5	23.68	18.24	15.13	12.26	35.07

II. Design of microfluidic device

Microfluidic chip separates sperm with high motility using rheotaxis and boundary-following behavior. Considering the optimized design, the overall dimensions of the butterfly-shaped chip are introduced in Table S3 according to Fig. S1.

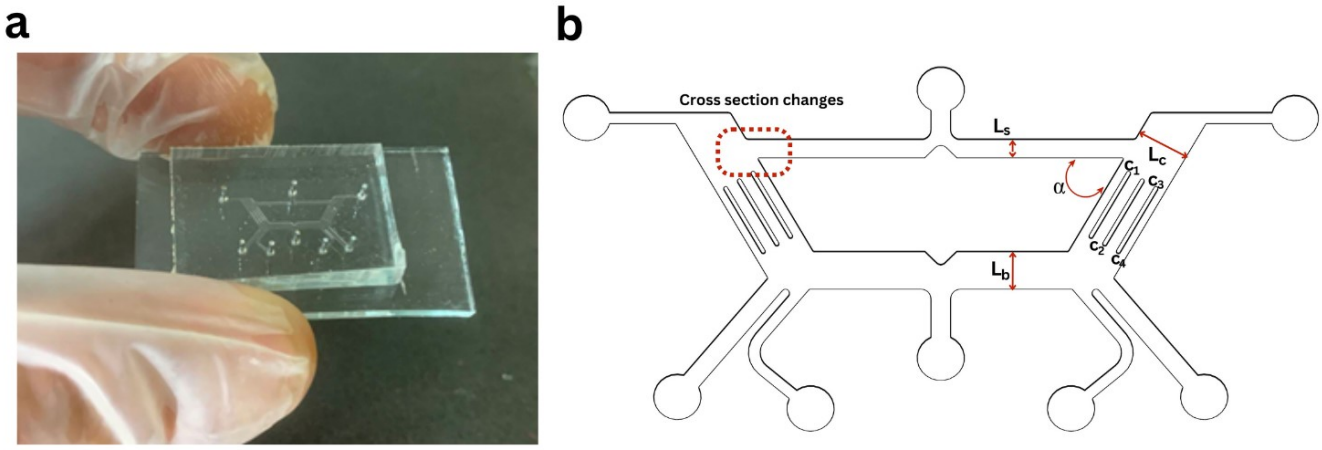

Figure S1. (a) Image of the butterfly-shaped microfluidic chip designed to isolate highly motile sperm. (b) Chip design parameters and cross-section changes.

Table S3. Dimensions of the BSC

Symbol	α	$C_{1(\mu m)}$	$C_{2(\mu m)}$	$C_{3(\mu m)}$	$C_{4(\mu m)}$	$L_{s(\mu m)}$	$L_{b(\mu m)}$	$L_{c(\mu m)}$
Value	60°	250	300	300	200	500	1000	1350

Increasing the buffer flow rate leads to an increase in velocity in the guiding arrays, which can serve as a barrier to the movement of sperm with low progressive motility. In addition, by increasing the sperm flow rate, a greater number of sperm with high progressive motility can be introduced into the guiding arrays, resulting in increased motility parameters in sperm.

Therefore, as shown in Fig. S2, simultaneous increases in buffer and sperm flow rate can serve as a filter allowing only sperm with high progressive motility to penetrate.

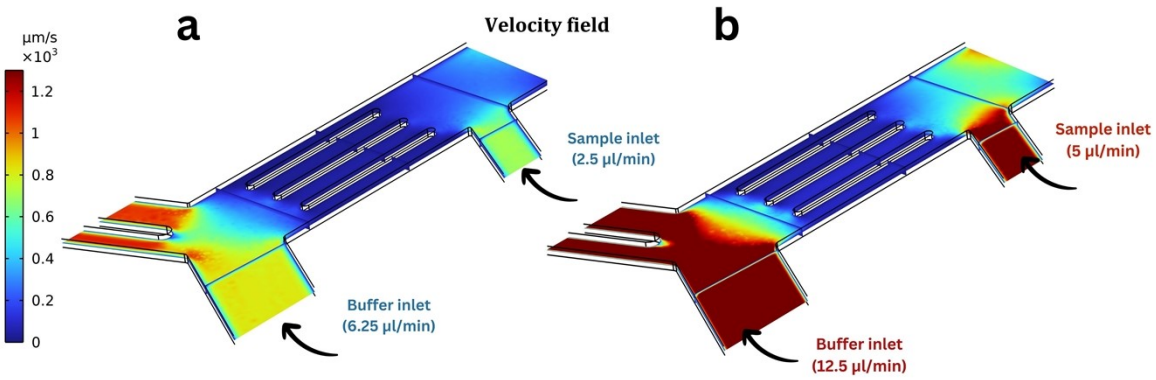

Figure S2. (a) The velocity field across the entire chip and guiding arrays provides an appropriate speed for the rotation and initiation of sperm rheotaxis (b) Increasing buffer and sperm flow rates (5) enhances velocity within the rheotaxis zone, leading to the dominance of inertial forces.

As the concentration increases, the number of sperm entering the rheotaxis zone also rises, leading to a higher separation rate. This increase continues until the high concentration impedes the movement and rotation of motile sperm. As a result, at higher concentrations, motile sperm lose their ability to exhibit rheotaxis movement due to collisions with other particles (Table S4).

Table S4. Sperm separated from the channel C1 within 20 minutes.

Experiment	Concentration (10^6 Sperm cells/mL)	Separation rate (In 20 minutes in C1)
1	20	530
2	40	785
3	60	1580
4	80	2400
5	100	1300
6	120	1150

III. Sperm DNA fragmentation

The following equation is used to calculate the sperm DNA fragmentation percentage:

$$\text{SDF (\%)} = \frac{\text{Number of fragmented sperm}}{\text{Total number of sperm}} \times 100 \quad \text{(S4)}$$

Sperm without halos and small halos are sperm with damaged DNA structures. Sperm with medium and large halos have a healthy DNA structure (Fig. S3).

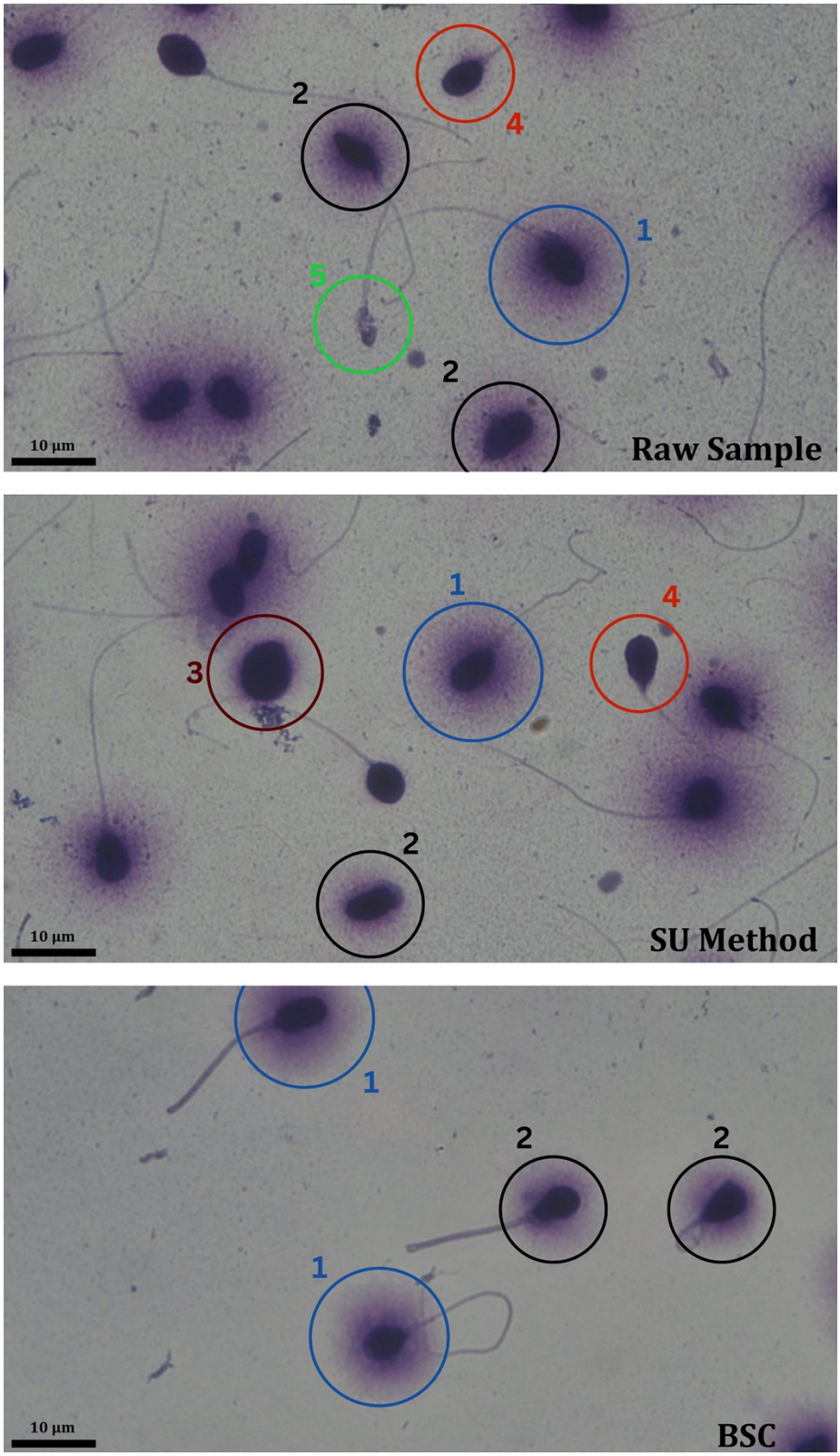

Figure S3. The image illustrates the sperm chromatin dispersion test in three different methods. Unfragmented: 1-Sperm cell with a large halo. 2-Sperm cell with a medium-sized halo. Fragmented: 3-Sperm cell with a small halo (halo width less than 1/3 of the small head diameter of the sperm). 4-Sperm cell without a halo. 5-Degraded sperm

For 10 different semen samples, the values of the sperm's biological parameters are as shown in the table below.

Table S5. Biological and motility sperm parameters of semen samples.

Sample	Total motility(%)	Immotile Sperm(%)	Concentration (10^6 Sperm cells/mL)	SDF(%)
1	51.5	48.5	124	13.1
2	48.9	51.1	69	17.5
3	43.08	56.92	158	19.6
4	44.9	55.1	97	11.2
5	64.6	35.4	101	16.3
6	41.01	58.99	132	23.2
7	46.7	53.3	62	20.7
8	51.04	48.96	80	18
9	46.5	53.5	138	16.3
10	60.3	39.7	118	18.8
Average	49.8±7.1%	50.2±7.1%	107.9±29.9%	17.47±3.95 %

The percentage of motility and biological parameters for the raw sample and two separation methods, the BSC and SU method, are displayed in Table S6.

Table S6. Biological and motility parameters of sperm

Sperm sample parameters	RAW	SU method	BSC
Total motility (%)	49.8	74.2	95.9
SDF (%)	17.4	10.7	3.4
Progressive Motility (Grade A)	15.3	22.7	66.9
Progressive Motility (Grade B)	15.1	28.2	28
VCL ($\mu m\ s^{-1}$)	31.2	49.2	77.4

Nomenclature:

ART	Assisted reproduction technology
WHO	World Health Organization
IVF	In vitro Fertilization
ICSI	Intracytoplasmic sperm injection
DGC	Density-gradient centrifugation
SDF	Sperm DNA Fragmentation
BSC	Butterfly-Shaped Chip

Supplementary movies:

Movie S1. Trajectories of the motile sperm undergoing rheotaxis and showing boundary-following behavior, and those not motile enough to overcome the flow, and enter the buffer flow (Black streamlines sperm flow and orange streamlines buffer flow).

https://drive.google.com/file/d/1OhadXPSHIujQcHVr-Oh3sVaUq8Lm9wy6/view

Movie S2. Sperm separation at a concentration of 80 million sperm per mL and a flow rate of 2.5 µL min^{-1}. The blue circle indicates the motile sperm, which can move through the buffer flow and enter the guiding array due to its progressive motility (high-motility sperm). The red circle indicates sperm that are unable to enter the guiding array due to their low swimming speed (low-motility sperm).

https://drive.google.com/file/d/1GubwEeTey4Lw7667WSzq39SCC80u1G1V/view?usp=drive_link

Movie S3. By increasing the concentration to 100 million sperm per mL at a flow rate of 2.5 µL min^{-1}, sperm collide with each other due to the increase in concentration and prevent the movement of motile sperm towards the outlet (red and black circle).

https://drive.google.com/file/d/1Tvknnf5AMh3E8CZHerk1oIJz1nV2GiM7/view

Movie S4. Sperm separation in Channel 4 (C4) at a flow rate of 2.5 µL min^{-1} and concentration of 80 million sperm per mL.

https://drive.google.com/file/d/17Hr67u_o6PYAmZpxOIl2h1eDIgM1_PcI/view

Movie S5. The movement of sperms from the guiding arrays to the outlet.

https://drive.google.com/file/d/1W-sYPWjMVXAUCjklbaVPDzYR0vjsRYSB/view

Movie S6. At the buffer flow rate greater than 7.5 µL min^{-1}, sperm cannot penetrate the buffer flow due to the high velocity of the flow.

https://drive.google.com/file/d/1YoQJBQUpRP0hgLL2h3XtzSrEdb8VIFhc/view

References

1 I. R. Sarbandi, A. Lesani, M. Moghimi Zand, and R. Nosrati, *Sci. Rep.*, 2021, **11**, 18327.

2 S. Sharma, M. A. Kabir, and W. Asghar, *Analyst*, 2022, **147**, 1589–1597.

3 S. A. Vasilescu, L. Ding, F. Y. Parast, R. Nosrati, and M. E. Warkiani, *Microsystems Nanoeng.*, 2023, **9**, 37.

4 M. Zaferani, S. H. Cheong, and A. Abbaspourrad, *Proc. Natl. Acad. Sci. U. S. A.*, 2018, **115**, 8272–8277.

5 J.-K. Wu, P.-C. Chen, Y.-N. Lin, C.-W. Wang, L.-C. Pan, and F.-G. Tseng, *Analyst*, 2017, **142**, 938–944.

6 A. Heydari, M. Zabetian Targhi, I. Halvaei, and R. Nosrati, *Sci. Rep.*, 2023, **13**, 1185.

7 S. Tasoglu, H. Safaee, X. Zhang, J. L. Kingsley, P. N. Catalano, U. A. Gurkan, A. Nureddin, E. Kayaalp, R. M. Anchan, R. L. Maas, E. Tüzel, and U. Demirci, *Small*, 2013, **9**, 3374–3384.